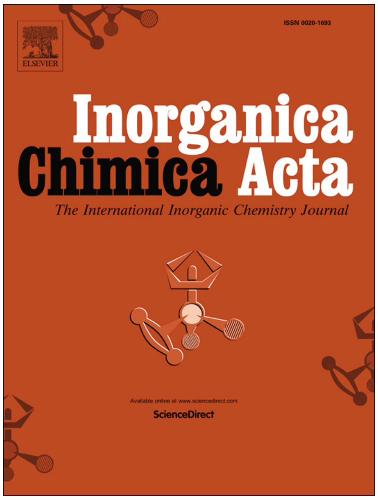

Research paper

Pd(II) porphyrins: Synthesis, singlet oxygen generation and photoassisted oxidation of aldehydes to carboxilic acids

Vijayalakshmi Pandey, Drishti Jain, Nitesh Pareekh, Iti Gupta

PII: S0020-1693(19)31211-3
DOI: https://doi.org/10.1016/j.ica.2019.119339
Reference: ICA 119339

To appear in: *Inorganica Chimica Acta*

Received Date: 16 August 2019
Revised Date: 29 November 2019
Accepted Date: 2 December 2019

Please cite this article as: V. Pandey, D. Jain, N. Pareekh, I. Gupta, Pd(II) porphyrins: Synthesis, singlet oxygen generation and photoassisted oxidation of aldehydes to carboxilic acids, *Inorganica Chimica Acta* (2019), doi: https://doi.org/10.1016/j.ica.2019.119339

Pd(II) porphyrins: Synthesis, singlet oxygen generation and photoassisted oxidation of aldehydes to carboxilic acids

Vijayalakshmi Pandey,[a] Drishti Jain,[a] Nitesh Pareekh[a] and Iti Gupta*[a]

Indian Institute of Technology Gandhinagar, Village Palaj, Simkheda, Gandhinagar,
Gujarat-382355, India. *Corresponding author, e-mail: iti@iitgn.ac.in

Graphical Abstract

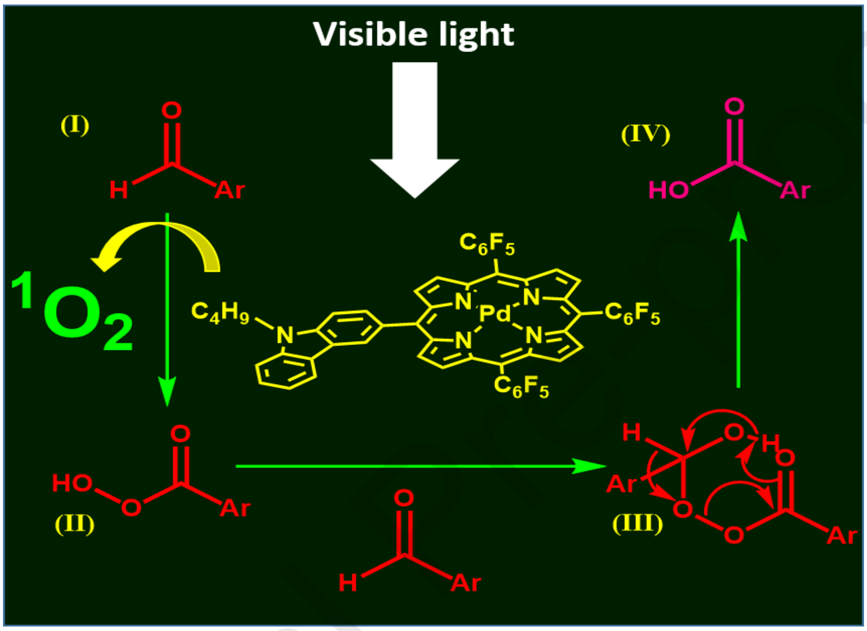

The synthesis and spectral studies of A_3B and A_2B_2 type porphyrins and their Pd(II) complexes are reported. The *meso*-positions on porphyrin macrocycle are substituted with pentafluorophenyl and *N*-butylcarbazole or triphenylamine groups. Pd(II) porphyrins displayed decent phosphorescence ~670 nm and are able to produce singlet oxygen by type II pathway, after photoirradiation. The calculated singlet oxygen quantum yields for Pd(II) porphyrins are ($\Phi_\Delta =$ 30% to 63%). The catalytic application of Pd(II) porphyrins towards photoassisted aerobic oxidation of aromatic aldehydes to carboxylic acids is demonstrated.

Keywords: Singlet oxygen, Photosensitizer, Palladium porphyrins, Catalyst, Oxidation

Introduction

Porphyrins are a class of naturally occurring pigments, found in biomolecules like: haemoglobin, chlorophyll and cytochrome P450 [1,2]. Metalloporphyrins, are well known prosthetic groups present in the various proteins and enzymes; and they are responsible for the catalytic activities of these biomolecules [3]. In recent years, metalloporphyrins have been developed as important synthetic tools for organic transformations. Ruthenium, iron, manganese complexes of porphyrins are used as efficient catalyst for C-H oxidations with high selectivity and good product yields [4,5]. Cobalt(II) porphyrin is used for the industrial scale bioinspired oxidation of cyclohexane to cyclohexanone [6]. Iron(III) and manganese (III) porphyrins are effectively used as catalysts for the epoxidation of alkenes by oxidizing reagents [7,8]. The dendritic ruthenim porphyrin was employed as catalyst for the epoxidation of chiral cholesteryl ester with high selectivity [9]. Transformation of primary alcohols to aldehydes is important for organic synthesis and catalytic oxidation with molecular oxygen was possible with the help of ruthenium (III) porphyrin catalyst [10]. The oxidation of hydrocarbons using molecular oxygen under mild conditions is still a challenging issue, as O_2 does not react with organic compounds due to spin rule [11]. The selective oxidations with oxygen can be achieved in the presence of free base porphyrins or metallporphyrins; because they are effective photosensitizers for singlet oxygen generation [12,13]. In this regard, porphyrin derivatives are noticeable photosensitizers owing to their high absorption coefficient, triplet excited states and high photostability. In fact, *meso*-tetraphenylporphyrin (H_2TPP) is one of the most effective photosensitizer for singlet oxygen generation [14]. *Meso*-aryl porphyrins and their zinc(II), iron(III), manganese(III), cobalt(II) complexes have been used as catalysts for the oxidation of cyclohexane and aromatic aldehydes by molecular oxygen in the presence of sunlight/light source [15-19]. The choice of central metal ion and the *meso*-aryl groups on porphyrin macrocycle can have significant role in their catalytic activity; and electron fluorinated aryl groups at the *meso*-position can have positive impact on catalytic photooxidation [15]. Keeping this in mind, we have prepared a series of A_3B and A_2B_2 type porphyrins bearing two or three C_6F_5 groups at the *meso*-positions and one or two electron donating bulky aromatic heterocycles (*N*-butylcarbazole or triphenylamine). Their palladium (II) complexes were prepared to test their potential as photosensitizers and catalysts for photooxidation of aromatic aldehydes.

In this work, synthesis and optical studies of A_3B and A_2B_2 type porphyrins and their Pd(II) complexes are reported. The *meso*-positions on porphyrin macrocycle are substituted with pentafluorophenyl and *N*-butylcarbazole or triphenylamine groups. Phosphorescence emission and singlet oxygen generation studies of Pd(II) porphyrins is also reported. The TD-DFT calculations are performed to understand the absorption properties of these molecules. Metalloporphyrins were also tested as catalysts for the photoassisted aerobic oxidation of aromatic aldehydes to carboxylic acids.

Results and Discussion

Synthesis and characterization

The synthetic strategy to make free base porphyrins and their Pd(II) complexes is shown in Scheme 1. In the first step, bulky heterocyclic aldehydes (9-butyl-9H-crbazole-3-carbaldehyde and/or 4-(diphenylamino)benzaldehyde) were condensed with 5-pentafluoro-phenyl-dipyrromethane in the presence of catalytic amount of TFA (trifluoroacetic acid). In the second step, crude mixture was oxidized by DDQ (2,3-dichloro-5,6-dicyano-1,4-benzoquinone) to produce the target porphyrins **1-4**. The desired A_2B_2-porphyrins (**1** and **3**) were isolated in decent yields (15–16%) after the neutral alumina column chromatography [20]. The scrambling of dipyrromethane also resulted in the formation of corresponding A_3B type porphyrins (**2** and **4**). Again purification of the crude reaction mixture by neutral alumina column afforded **2** and **4** in reasonable yields (10-11%). Then, the synthesis of palladium complexes of porphyrins (Scheme 1) was performed by reacting the free base porphyrins **1-4** in DCM (dichloromethane) with $PdCl_2$ dissolved in methanol. The longer reaction time (~24 h) was required for the formation of the Pd(II) porphyrins because of the poor solubility of palladium salts. The crude products were subjected to neutral alumina column chromatography and pure metalloporphyrins **1Pd-4Pd** were obtained in 79-86% yields as orange solid.

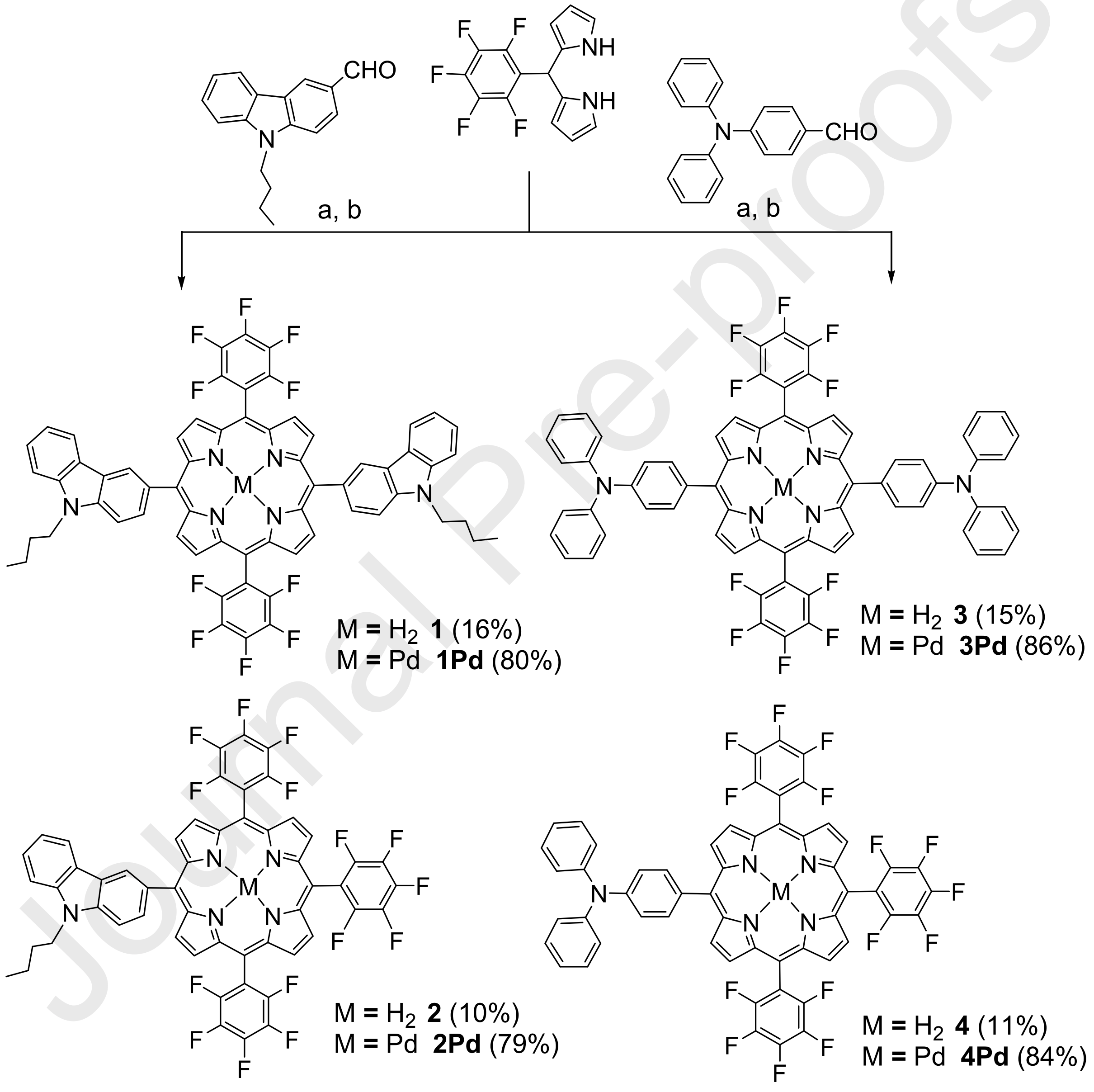

Scheme 1: Synthesis of free base porphyrins (**1-4**) and their Pd(II) complexes (**1Pd-4Pd**); a: DCM, TFA,4 h followed by DDQ, 2h, RT; b: DCM, $Pd(Cl)_2$, RT, 24h.

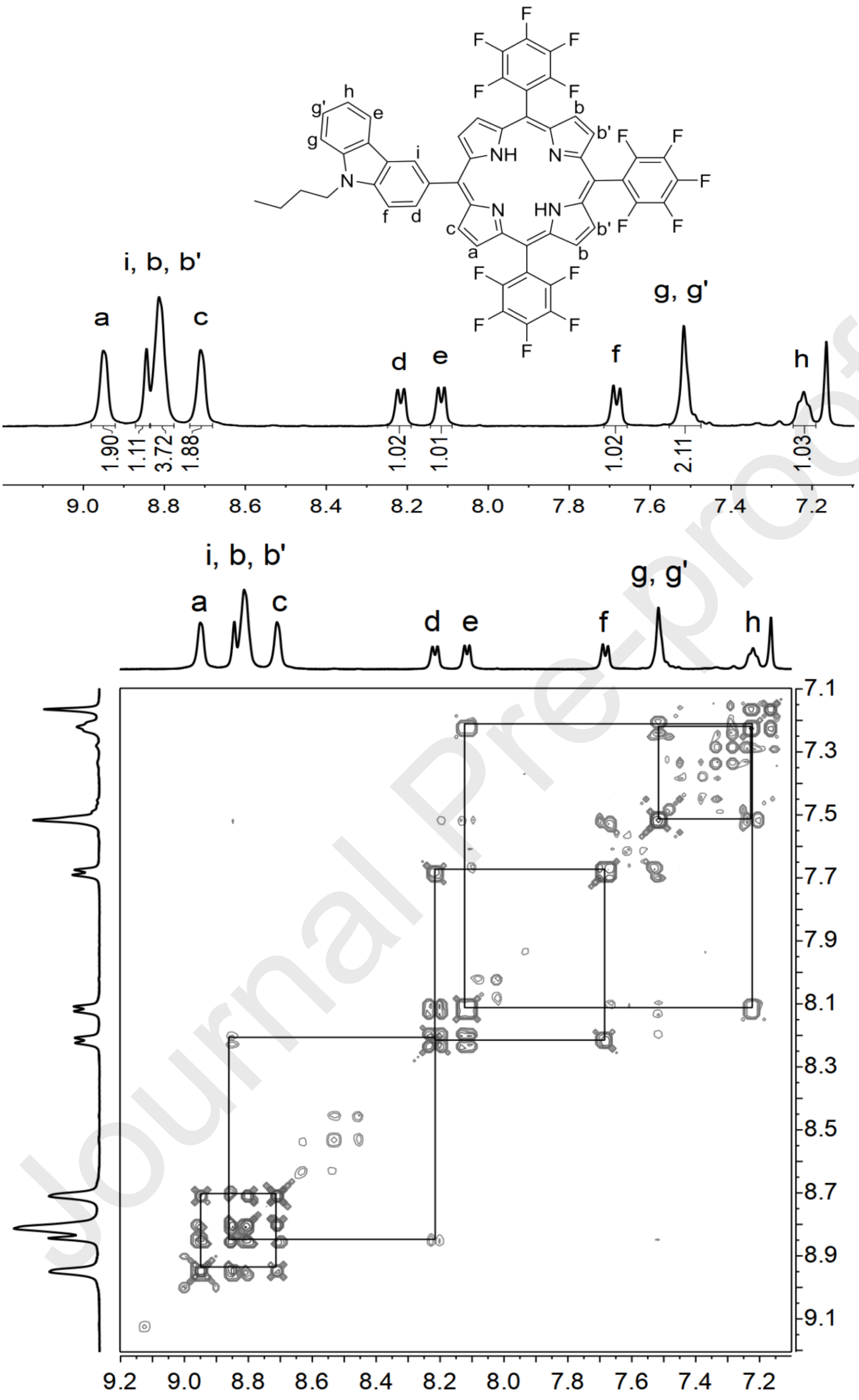

Figure 1. Partial ^{1}H NMR and ^{1}H-^{1}H COSY spectra of porphyrin **2** recorded in $CDCl_3$.

All the porphyrins were characterized by standard spectroscopic techniques *viz.* IR, ^{1}H-NMR,^{13}C-NMR and MALDI-TOF mass spectrometry (*cf.* supplementary information). The porphyrins **1, 3** and their corresponding metal complexes **1Pd** and **3Pd** have been reported previously [20]. The representative ^{1}H and HOMO-COSY spectra of porphyrin **2** (aromatic region) are shown in Figure 1. With the help of COSY spectrum, the structure of porphyrin **2** was identified; the eight β pyrrole protons showed up as three set of doublets between 8.95 and 8.71 ppm. The seven aryl protons of the *meso*-*N*-butylcarbazole group appeared between 8.22 to 7.16 ppm. The upfield signal at –2.81 ppm is characteristic of the two inner N-H protons of the aromatic porphyrin core (*cf.* SI). The signals at 4.50, 2.03, 1.56 and 0.81 ppm appeared for the butyl chain of *N*-butylcarbazole groups. In the cases of metalloporphyrins **1Pd-4Pd**, the disappearance of the characteristic upfield signal of inner N-H protons suggests the formation of palladium complexes. Furthermore, the corresponding molecular ion peak were also observed in the MALDI-mass spectra of the new porphyrins (**2**, **4, 2Pd** and **4Pd**) confirming their formation (*cf.* SI).

Absorption and Emission Studies

The UV-Vis absorption spectra of porphyrins and palladium porphyrins were recorded in toluene at room temperature; the absorption and emission data are presented in Table 1. All the porphyrins exhibited well defined, narrow absorption bands and the absorption data (Table 1) are consistent as per the literature reports [21,22]. The free base porphyrins **2** and **4** exhibited a strong Soret band at 419 nm range (Figure 2a), which is slightly broader than that of the H_2TPP [23]. The absorption pattern of four Q-bands is similar to H_2TPP, with negligible shifts in their absorption values; however, the Q3 band of both the porphyrins showed 12 nm red shifts as compared to that of the H_2TPP (548 nm).

Table 1. Photophysical studies data of porphyrins recorded in toluene; (Concentration = 2.4 x10^{-6}).

Porphyrin	λ_{abs} (nm) (ε x 10^{-3}) (M^{-1} cm^{-1})	λ_{ex} (nm)	λ_{em} (nm)	Φ_f
2	419 (218), 516 (14), 560 (0.2), 592 (0.8), 650 (0.5)	515	654, 716	0.065
4	415 (333), 518 (26), 560 (10), 595 (10), 652 (0.1)	515	659, 719	0.046
2Pd	413 (409), 526 (51), 559 (4)	413	561, 613, 665	---
4Pd	410 (293), 528 (36), 559 (5)	413	559, 611, 680	---

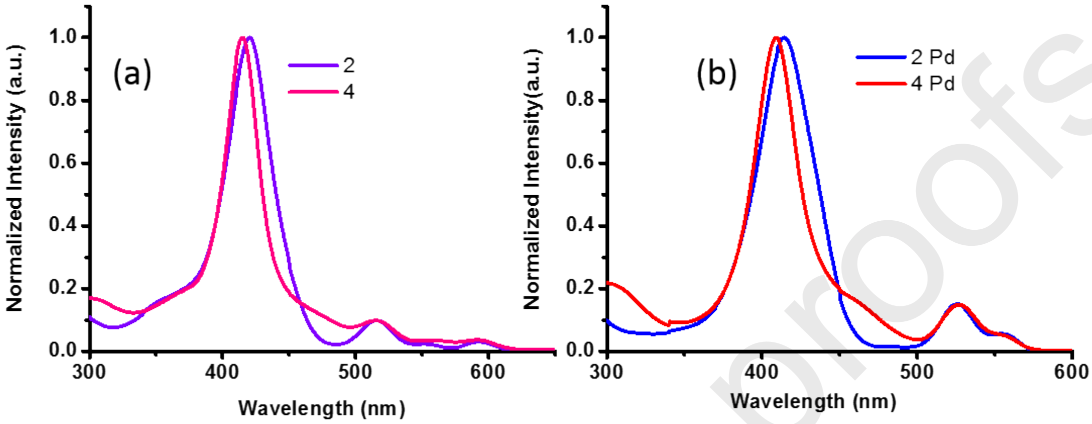

Figure 2. The comparision of absorption spectra of porphyrins, (a) **2** and **4**; (b) **2Pd** and **4Pd** recorded in toluene.

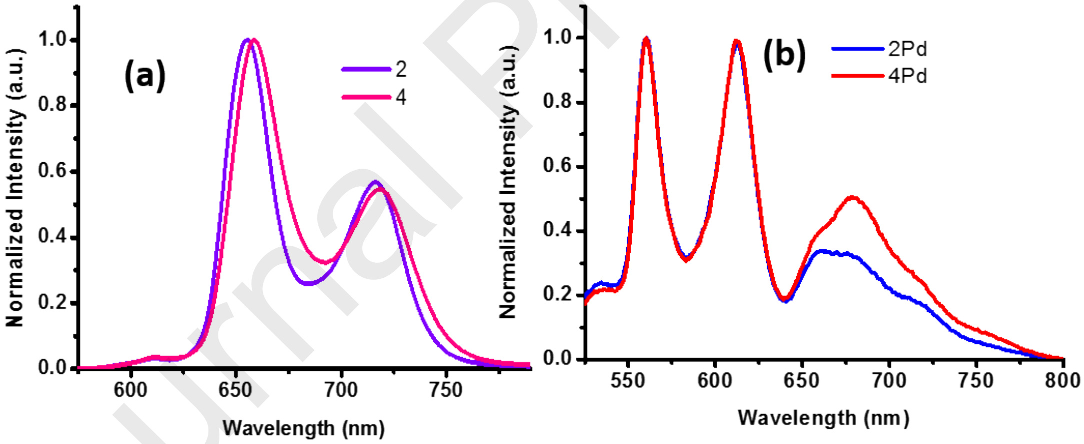

Figure 3. The comparison of emission spectra of porphyrins, (a) **2** and **4** (λ_{ex} = 515 nm); (b) **2Pd** and **4Pd** (λ_{ex} = 413 nm) recorded in toluene.

The palladium complex of porphyrins **2Pd** and **4Pd** exhibited three absorption bands (Figure 2b); the higher energy Soret band appeared at 413 nm and two Q bands between 526-559 nm (Table 1). The absorption spectra of **2Pd** and **4Pd** (A_3B type porphyrins) were similar to the previously reported A_2B_2 type Pd(II) porphyrins [20]; suggesting that one or two bulky heteroaromatic group on the *meso*-position have less significant effect on their electronic property. The fluorescence spectra of porphyrins **2** and **4** were recorded in toluene and the comparative emission spectra are shown in Figure 3a. The emission spectra of the porphyrins **2** and **4** exhibited two emission bands around 656 and 719 nm. The higher energy emission bands of **2** and **4** were 4–9 nm red-shifted as compared to that of the H_2TPP. The fluorescence quantum yields (Φ_f) of **2** and **4** were estimated from the emission and absorption spectra by comparative method, using standards H_2TPP ($\Phi_f = 0.11$) [23]. The fluorescence quantum yields of the porphyrins **2** and **4** (Table 1) were slightly lower than H_2TPP; which indicated noticeable nonradiative decay processes of their excited singlet states [24, 25]. Emissive properties of the Pd(II) porphyrins (**2Pd** and **4Pd**) were studied in the deaerated toluene; and the photoluminescence spectra of are shown in Figure 3b. The emission spectra showed one phosphorescence band of medium intensity for **2Pd** and **4Pd**; owing to the rapid singlet-triplet intersystem crossing in these Pd(II) porphyrins; two moderately intense fluorescence bands around 560 and 511 nm were also observed for **2Pd** and **4Pd** (Table 1). Significant phosphorescence was seen for **2Pd** and **4Pd**, as a result of palladium induced spin orbit coupling which promotes radiative decay from the triplet state (T_1). The observed phosphorescence bands in **2Pd** (665 nm) and **4Pd** (680 nm) were red shifted as compared to their corresponding lowest energy absorption peak (QI-band).

Computational Studies

Density Functional Theory (DFT) calculations were carried out to gain further insight about the electronic structure of the porphyrins **2**, **2Pd**, **4** and **4Pd**, using the CPCM-TD-B3LYP/6-311+(d) level of theory [26]. For palladium porphyrins 2Pd and 4Pd, LANL2D2 was used to generate effective core potential. The geometrical parameters and the gas phase optimized molecular structures of porphyrins **2**, **2Pd**, **4** and **4Pd** are provided in the supplementary information (Figures S11, S12). The DFT studies of **1**, **1Pd**, **3** and **3Pd** are reported in the previous work [20].

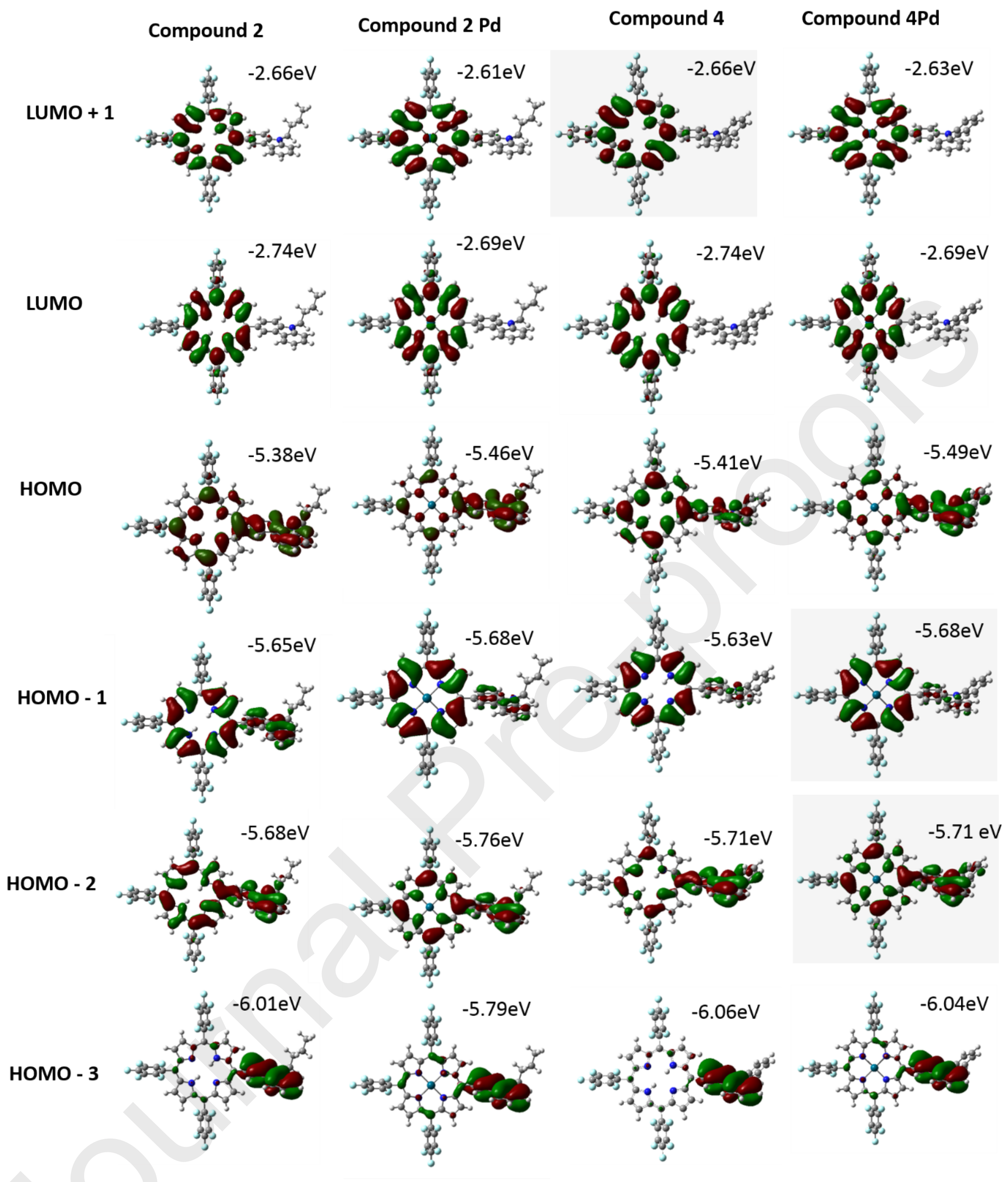

Figure 4. The Khon-Sham orbital representation of the frontier molecular orbitals and their corresponding energies of **2**, **2Pd**, **4** and **4Pd** at the CPCM-TD-B3LYP/6-311+(d) level of theory in gas phase.

The molecular orbitals of four porphyrins were produced both in the gas phase and in toluene with time-dependent density functional theory (TD-DFT) at B3LYP/6-31G+(d) level. The solvent effect of toluene was taken into account by the polarizable continuum model (PCM).

The frontier molecular orbitals involved in the electronic transitions for porphyrins **2**, **2Pd**, **4** and **4Pd** are presented in Figure 4. For the HOMO's of porphyrins **2**, **2Pd**, **4** and **4Pd**, the electron density was mainly localized on the aromatic heterocycles (*N*-butylcarbazole or triphenylamine) present on the *meso*-positions of the porphyrin ring (Figure 4). On the contrary, for LUMO energy levels the electron density was more concentrated on the porphyrin core. The role of excitation energies and frontier molecular orbitals in the absorption spectra of porphyrins **2**, **2Pd**, **4** and **4Pd** is clear from the data presented in table 2. For compounds **4** and **5** one major absorption band was obtained and its wavelength (λ_{abs}) was selected for comparison. The calculated λ_{abs} values for the absorption band of highest oscillatory strength, were 18 to 24 nm blue shifted as compared to the experimental values (Table 1); which could be due to limitation of vertical approximation. The maximum oscillatory strengths were in between 0.31 to 1.56 for the porphyrins studied here (Table 2). For free base porphyrins **2** and **4** the dominant electronic transitions were observed from HOMO-1 to LUMO+1 and HOMO-2 to LUMO level, respectively. In the case of palladium porphyrins **2Pd** and **4Pd** the major transitions were obtained from HOMO-5 to LUMO+1 and HOMO-3 to LUMO+1 level, respectively (Table 2). The DFT calculated HOMO-LUMO gaps for free base porphyrins **2** and **4** were 2.639 and 2.666 eV, respectively. Similarly, for **2Pd** and **4Pd** the values of HOMO-LUMO band were 2.775 and 2.802 eV, respectively. It is clear that, the HOMO-LUMO gaps of metallated porphyrins **2Pd** and **4Pd** are slightly higher than those of the corresponding freebase porphyrins **2** and **4**, respectively.

Table 2. Calculated electronic excitation energies, oscillator strengths, and eigenvectors for TD-DFT spectra of **2**, **2Pd**, **4** and **4Pd** using CPCM-TD-B3LYP/6-311+(d) level of approximation.

Molecule	Excited state energy (eV)	Contribution	Coefficient	λ (nm)	oscillatory strength (*f*)	Experimental λ_{abs} values in Toluene

2	3.11	HOMO→LUMO	8	397.95	1.56	422
		HOMO-1→LUMO+1	16			
		HOMO-1→LUMO	9			
		HOMO-1→LUMO+1	6			
		HOMO→LUMO	4			
		HOMO-1→LUMO+1	1			
2Pd	3.12	HOMO-6→LUMO	2	396.45	0.31	415
		HOMO-5→LUMO+1	24			
		HOMO-4→LUMO	6			
		HOMO-4→LUMO+1	1			
		HOMO-3→LUMO	6			
		HOMO-3→LUMO+1	1			
		HOMO-2→LUMO	3			
		HOMO-1→LUMO+1	4			
4	3.14	HOMO-3→LUMO	7	394.40	1.53	413
		HOMO-2→LUMO	1			
		HOMO-2→LUMO+1	13			
		HOMO-1→LUMO	8			
		HOMO-1→LUMO+1	9			
		HOMO→LUMO	5			
		HOMO→LUMO+1	1			
4Pd	3.16	HOMO-3→LUMO	7	391.38	1.20	410
		HOMO-3→LUMO+1	1			
		HOMO-2→LUMO	1			
		HOMO-2→LUMO+1	17			
		HOMO-1→LUMO	12			
		HOMO-1→LUMO+1	2			
		HOMO→LUMO+1	2			

Singlet Oxygen Generation

The production of singlet oxygen ($^1O_2$) upon irradiation of the photosensitizers has potential applications in the PDT (photo-dynamic therapy) of tumors and DNA damage [27,28]. Typically, $^1O_2$ is thought to be the dominant cytotoxic species in the PDT studies of porphyrin-based photosensitizers [29]. Metalloporphyrins containing heavy metals like platinum and palladium at the core are known to exhibit considerably high inter-system crossing (ISC) due to heavy atom effect. The augmented ISC results in the sufficiently populated triplet excited states of the metalloporphyrins, and they can generate $^1O_2$ by type II pathway; which involves energy transfer from porphyrin’s triplet state to the ground state molecular oxygen (triplet) [28]. Metalloporphyrins have also been utilized as catalysts for the photooxidation of alcohols and alkenes, owing to their ability to generate singlet oxygen [15-17].

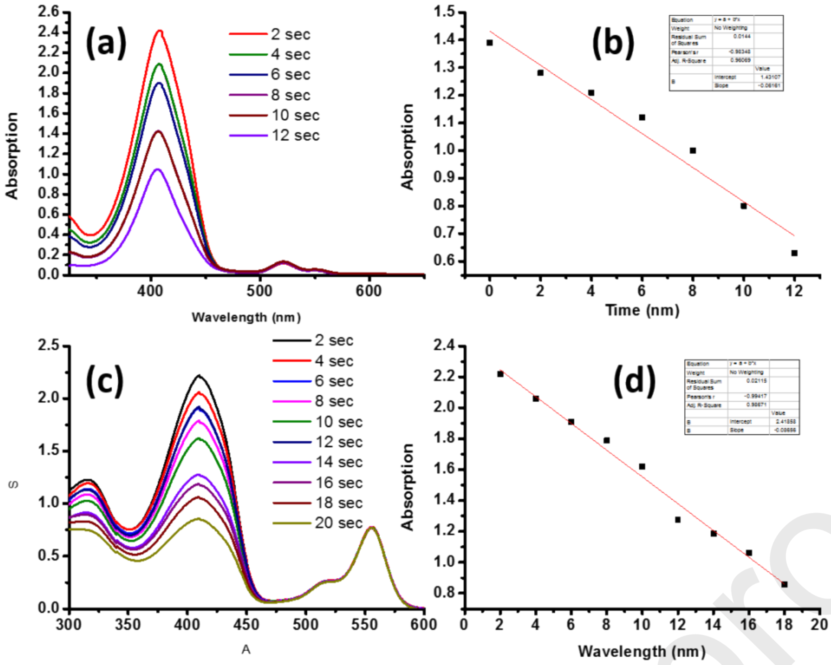

Figure 5. UV-vis spectral changes in (a) porphyrin **2Pd** and (c) Rose Bengal in $CHCl_3$ on photoirradiation (λ = 365 nm, 21 J cm^{-2}); the rate of decrease in absorption measured at 324 nm for (b) **2Pd** and (d) Rose Bengal.

Table 3. Absorption and singlet oxygen generation data of Pd(II) porphyrins in different solvents.

Pd(II) Porphyrins	Solvents	λ_{abs} (nm) (ε x 10^{-4} to 10^{-5}) (M^{-1} cm^{-1})	$^1O_2$ %
1Pd	Chloroform	424 (688), 526 (98), 560 (023)	46
2Pd	Chloroform	407 (709), 527 (121), 561 (042)	50
3Pd	Chloroform	404 (682), 522 (95), 553 (022)	35
4Pd	Chloroform	401 (725), 521 (118), 554 (041)	58
1Pd	Acetonitrile	407 (800), 521 (122), 556 (055)	38
2Pd	Acetonitrile	402 (803), 525 (137), 561 (054)	54
3Pd	Acetonitrile	404 (819), 522 (110), 553 (042)	30
4Pd	Acetonitrile	401 (802), 520 (138), 554 (043)	56
2Pd	Dimethylformamide	405 (805), 526 (125), 560 (045)	49
2Pd	Tetrahydrofuran	404 (781), 524 (126), 555 (042)	63

The singlet oxygen quantum yields of palladium porphyrins (**1Pd**, **3Pd** and **4Pd**) were examined in two solvents chloroform and acetonitrile; oxygen gas was purged in the UV-cell before measurement of the absorption intensity of the compounds (*cf* ESI). The 1,3-diphenylisobenzofuran (DPBF) was used as oxygen scavenger in the solution and singlet oxygen generation by Pd(II) porphyrin was monitored by UV-vis spectrometer [30]. In this assay Rose Bengal was used as a reference compound [31]. The significant inter-system crossing (ISC) would lead to the energy transfer from photosensitizers (**1Pd-4Pd**) to triplet ground state of oxygen molecules; which in turn get excited to singlet state and react with DPBF. The decrease in the intensity of DPBF absorption band at 324 nm was monitored over a time period of ~2 minutes. For photo-irradiation of the porphyrins UVA light source ($\lambda = 365$ nm, 21 J cm^{-2}) was used; as the time progressed the intensity of the DPBF absorption band at 324 nm gradually decreased (Figure 5a). The triplet photosensitization ability of the porphyrin **2Pd** was compared with the reference photosensitizer (Rose Bengal, $\Phi_\Delta = 0.56$ in acetonitrile) under similar conditions (Figure 5c). The obtained absorption data were fitted to equation 1 to calculate the values of singlet oxygen quantum yield [32]. The plots of singlet oxygen studies for the rest of the porphyrins are provided in the supplementary information (Figures S8-S13). The singlet oxygen quantum yield, calculated for Pd(II) porphyrin **2Pd** was 54% in acetonitrile; and for the rest of the porphyrins (**1Pd, 3Pd** and **4Pd**) it was in the range of 30-56% (Table 3). Also, in chloroform the singlet oxygen quantum yields of the Pd(II) porphyrins were in the range of 35-58 (Table 3). The studies indicated that these porphyrins can be effectively used as catalysts for photooxidation of organic compounds.

Catalytic Photooxidation of Aldehydes

The free base porphyrins and metalloporphyrins are known for their catalytic properties; porphyrin derivatives have been used as photocatalysts for the oxidation of aldehydes, alkene and alcohols [4]. Typically, singlet oxygen can be generated by chemical method or by photosensitized reaction in the presence of light. The photochemical method to generate singlet oxygen is quite cost-effective and porphyrin derivatives are known to produce $^1O_2$, by energy transfer to the molecular oxygen. This $^1O_2$ can be utilized further to oxidize the organic compounds /hydrocarbons under aerobic conditions. Previous report by Safari and co-workers have used Pt(II) complexes of *meso*-tetraaryl porphyrins as efficient photocatalyst for similar organic transformations [32]. The group has used Pt(II) porphyrins for the aerobic oxidation of aldehydes in 16-87% yields (of carboxylic acids) [32]. However, synthesis of Pt(II) porphyrins is not easy and the cost of platinum salt is also high; thus, we tested the application of Pd(II) porphyrins as catalyst for oxidation reaction in the presence of light. The potential of palladium porphyrins (**1Pd-4Pd**) as catalyst for the photooxidation of aromatic aldehydes was investigated in a series of experiments, discussed *vide infra*. Four aromatic aldehydes: *p*-tolualdehyde, mesitaldehdye, *o*-nitrobenzaldehyde and *p*-nitrobenzaldehyde were selected as substrate. Initially, palladium porphyrin **2Pd** was used as catalyst to optimize the solvent for the aerobic oxidation of *o*-nitrobenzaldehyde in the presence of light. As per the literature, water, dimethylformamide, and dimethylsulfoxide are singlet oxygen quenchers; thus the yield of oxidized product can get affected [33]. It is clear from the Table 4 that, maximum yield of the *o*-nitrobenzoic acid was achieved when acetonitrile was used as solvent. Owing to its polar nature, acetonitrile can dissolve the variety of substrates and the catalysts and it is relatively inert toward oxidation; thus, it is good solvent for oxidation reactions.

Table 4: Effect of solvent on the photooxidation of 2-nitrobenzaldehyde to corresponding acid in the presence of catalyst **2Pd** and O_2.

Solvent	Yield of carboxylic acid	$^1O_2$ yield
Chloroform	31%	50%
Dimethylformamide	87%	49%
Tetrahyrdofuran	50%	63%
Acetonitrile	98%	56%

As per the data presented in Table 5, four palladium porphyrins (**1Pd-4Pd**) were used for the aerobic oxidation of aromatic aldehydes in the presence of light source (λ = 400-700 nm, 15 J cm^{-2}) at room temperature. The conversion took 24h in the presence of A_3B type porphyrins (**2Pd** and **4Pd**); whereas, photocatalytic reaction was extended to 36h in the case of A_2B_2 type porphyrins (**1Pd** and **3Pd**). The central metal ion of porphyrin ring and the *meso*-substituents have significant effect on the yield of carboxylic acid; as per the literature reports, paramagnetic metals like Fe(II) and Mn(II) show very short triplet state life time in solution and thus conversion was negligible [15]. Previous reports by Safari and co-workers showed that, the Zn(II) and Ni(II) porphyrins are less effective for such oxidation reactions; further Pd(II) porphyrins were also found to be less reactive for similar conversion [15, 32].

Table 5. Photooxidation of aldehydes to carboxylic acids in the presence of catalyst and O_2 in CH_3CN.

		(% Yield of Acid)			
		Porphyrin Catalyst			
Aldehyde	Carboxylic Acid	**1Pd**	**2Pd**	**3Pd**	**4Pd**
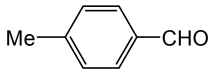	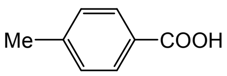	20%	17%	18%	53%
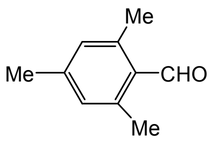	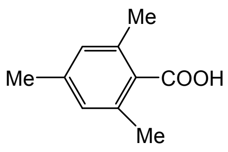	57%	61%	46%	71%
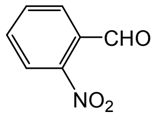	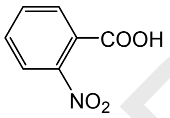	20%	98%	91%	15%
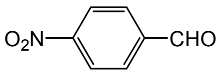		73%	73%	40%	34%

The Pt(II) porphyrins exhibit good fluorescence and phosphorescence, with sufficiently long triplet state lifetimes. In the presence of sunlight, Pt(II)porphyrin were employed as catalysts by Safari and co-workers for the conversion of *o*-nitrobenzaldehyde and *p*-nitrobenzaldehyde into their corresponding carboxylic acids; conversion yields were 83% and 69%, respectively [32]. It is clear from Table 5 that, Pd(II) porphyrins (**1Pd-4Pd**) can be used as efficient catalyst for the photoassisted oxidation of aldehydes. The yield of carboxylic acids were moderate 17% -71%, when electron donating groups were present on the benzene ring (*p*-tolualdehyde and mesitaldehyde); and **4Pd** gave relatively higher conversion yield. However, when electron withdrawing groups were present on the benzene ring (*o*-nitrobenzaldehyde and *p*-nitrobenzaldehyde) the good conversion yields (91-98%) were obtained with **2Pd** and **3Pd** catalysts, under similar conditions. These observations clearly suggest that, Pd(II) porphyrins reported in this work can be used as potential catalyst for such photooxidation of organic compounds.

Conclusions

A series of A_3B and A_2B_2 type porphyrins and their Pd(II) complexes are synthesized and characterized. Absorption and emission spectra of the A_3B type porphyrins showed standard pattern, similar to the parent porphyrins H_2TPP/ PdTPP. The Pd(II) complexes of A_3B type porphyrins, exhibited moderate phosphorescence peak (~670 nm) along with fluorescence peaks in the emission spectra. Due to heavy metal effect, Pd(II) complexes of A_3B type porphyrins were able to generate decent singlet oxygen (30-63%); which was further used for the oxidation of aromatic aldehydes into carboxylic acids. The conversion of *o*-nitrobenzaldehyde to its acid was achieved in high yields (91-98%); suggesting that Pd(II) porphyrins have good potential as catalyst for photoassisted oxidation reactions.

Acknowledgements

The financial support from IIT Gandhinagar is greatly acknowledged. VP is grateful to IIT Gandhinagar for fellowship and infrastructural support.

Supporting Information

The characterization data like ^{1}H and ^{13}C NMR, MALDI-MS spectra of selected porphyrins have been provided. Data for the singlet oxygen quantum yields of the selected molecules have also been provided. Geometry optimization data obtained from DFT calculation are also provided.

Experimental

Instrumentation and Reagents

Unless otherwise mentioned, all the reagents and solvents were purchased from Aldrich, or Acros Organics and used without further purification. Silica gel (100-140 mesh) from Merck was used for column chromatography. The NMR spectra of compounds were recorded with Bruker Avance III 500 MHz NMR spectrometer. MALDI mass spectra of compounds were UltrafleXtreme MALDI TOF/TOF (Bruker Daltonics). IR spectra of samples were recorded on Perkin Elmer L1600300 Spectrum TWO LITA. Absorption spectra were recorded with UV-1700 (Shimadzu, Japan). Fluorescence emission measurements were recorded with Horiba-Jobin Yvon Fluorlog-3 spectrometer (France). The synthesis of porphyrins **1, 3, 1Pd** and **3Pd** were reported in our previous work [20].

Computational Analysis

Density functional theory (DFT) and time-dependent density functional theory (TD-DFT) calculations of the four porphryins (**2**, **2Pd**, **4** and **4Pd**) were carried out the at CPCM-TD-B3LYP/6-311+(d) level [26]. The gas phase optimisation of all the free base porphyrins was carried out using 6-31G(d) basis sets. In the case of metalloporphyrins, 6-31G(d) basis was employed for non-metals and SDD[21] basis set was used for zinc and palladium metals. Absorption spectra of all these dyads were simulated with TD-DFT using B3LYP functional and the same basis sets. Gaussian 09[22] was used for all calculations. Frequency analysis confirmed the absence of imaginary frequencies. Theoretically, the intensity of the band is expressed regarding the oscillator strengths (f).

DFT calculations

The ground state geometry optimization of the molecules **2**, **2Pd**, **4** and **4Pd** were performed with density functional theory (DFT) at CPCM-TD-B3LYP/6-311+(d) level, using Gaussian

09 program package [21]. The vertical excitation energies were calculated employing time dependent density functional theory (TD-DFT) approach at the same functional and basis set.

Singlet Oxygen Quantum Yield

DPBF with a fixed concentration of (10^{-5}M) was prepared in dark and was covered with aluminium foil to avoid any kind of light exposure. By making effective concentrations of Rose Bengal (10^{-6} M) and all other compounds were recorded for absorption. Readings for Rose Bengal along with all other compound were recorded and the absorption decay was plotted at 410 nm to get the slopes. Following equation was used to calculate singlet oxygen quantum yield: $\phi_{\Delta(S)} = \phi_{\Delta(S0)}$ x {Slope(S) / Slope (S0)}; where S is the slope obtained from compounds and S_O is slope obtained from the standard compound.

General synthesis of Free base porphyrins

Aldehyde (100 mmol) and dipyrromethane (200 mmol) were dissolved in DCM (40 mL) and stirred for 2 mins followed by the addition of trifluoroacetic acid (5 µL). The reaction mixture was stirred under inert atmosphere for 4h, at room temperature in dark. After that, 2,3-dichloro-5,6-dicyano-1,4-benzoquinone (DDQ, 300 mmol) was added and reaction mixture was stirred for another 3h under air. Formation of the desired porphyrin was identified by observation of maroon colour spot on TLC (in 30% DCM/hexane). The crude reaction mixture was subjected to silica gel column to filter off excess DDQ and other oligomeric products using 100% DCM. Further purification was carried out with a neutral alumina column chromatography and the desired porphyrins were eluted with 20–30% DCM/hexane.

Porphyrin 2: Purple crystal, M.P >195 ^{O}C. Yield 10% (30 mg). mp. $R_f = 0.30$ (DCM/ Hexane 1: 1.2), MALDI-MS for $C_{54}H_{27}F_{15}N_5$ $[M+H]^+$ calcd 1030.2027 observed *m/z* 1030.32**.** IR (neat, cm^{-1}): 3319, 2950, 2928, 2859, 1594. ^{1}H NMR (500 MHz, Chloroform-*d*): δ (in ppm) –2.80 (s, 2H), 1.01 (t, *J* = 7.4 Hz, 3H), 1.53 (d, *J* = 7.4 Hz, 2H), 1.53 (d, *J* = 7.4 Hz, 2H), 4.47 (t, *J* = 7.2 Hz, 2H), 7.22 (t, *J* = 7Hz, 1H), 7.51 (s, 2H), 7.68 (d, *J* = 5 Hz, 1H), 8.12 (d, *J* = 7.5 Hz, 1H), 8.22 (d, *J* = 1.5 Hz, 1H), 8.71 (d, *J* = 4.5 Hz, 2H), 8.81 (m, 4H), 8.47 (s, 1H), 8.95 (d, *J* = 4.5 Hz, 2H); ^{13}C-NMR (125 MHz, Chloroform-*d*): δ (in ppm) 12.98, 13.08, 19.76, 21.66, 28.34, 28.67, 29.18, 30.37, 30.90, 30.31, 42.31, 100.47, 101.90, 105.86, 108.12, 118.39, 119.37, 120.72, 121.62, 123.70, 125.30, 125.86, 128.67, 130.45, 131.67, 139.33, 140.41, 144.57.

Porphyrin 4: Purple crystal, M.P >195^{O}C .Yield 15% (25 mg). M.P 195-205 ^{O}C. R_f = 0.33 (DCM/ Hexane 1: 1.2), MALDI-MS for $C_{56}H_{25}F_{15}N_5$ $[M+H]^+$ calcd 1052.1870 observed *m/z* 1052.58**.** IR (neat, cm^{-1}): 3309, 2959, 2916, 2848, 1593. ^{1}H-NMR (500 MHz, Chloroform-*d*): δ (in ppm) –2.86 (s, 2H), 7.07 (m, 4H), 7.38 (d, *J* = 8.4 Hz, 2H), 7.96 (d, *J* = 8.4 Hz, 2H), 8.74 (m, 4H), 9.02 (d, *J* = 4.7 Hz, 2H); ^{13}C-NMR (125 MHz, Chloroform-*d*): δ (in ppm) 100.55, 101.90, 114.92, 115.08, 119.74, 122.57, 122.57, 124.23, 128.58, 133.11, 134.67, 135.51, 137.51, 142.17

General synthesis of Pd(II) porphyrins

Porphyrin (0.01 mmol) was dissolved in DCM (20 mL) and palladium(II) chloride (0.04 g) dissolved in methanol (25 mL) was added to it. The reaction mixture was stirred for 24 hrs under inert condition. The formation of the desired product was identified by observation of orange colour spot on TLC (80% DCM/hexane), where the Pd(II) porphyrin appear more polar as compared to the starting porphyrin. The desired palladium porphyrins were further purified by neutral alumina column chromatography, using 90% DCM/hexane as solvent.

Porphyrin 2Pd: Orange solid, M.P. > 250 ^{O}C. Yield 79% (16 mg). R_f = 0.26 (DCM/ Hexane 1: 1.2), MALDI-MS for $C_{54}H_{25}F_{15}N_5Pd$ $[M+H]^+$ calcd 1134.0905 observed *m/z* 1134.38**.** IR (neat, cm^{-1}): 2949, 2930, 2862, 1580. ^{1}H NMR (500 MHz, Chloroform-*d*): δ (in ppm) 1.01 (t, *J* = 7.4 Hz, 3H), 1.55 (d, *J* = 7.4 Hz, 2H), 2.03 (t, *J* = 8 Hz, 2H), 4.50 (t, *J* = 7.2 Hz, 2H), 7.23 (t, *J* = 7Hz, 1H), 7.53 (t, *J* = 8.5 Hz, 2H), 7.67 (d, *J* = 5 Hz, 1H), 8.10 (d, *J* = 7.5 Hz, 1H), 8.18 (d, *J* = 1.5 Hz, 1H), 8.68 (d, *J* = 4.5 Hz, 2H), 8.78 (m, 4H), 8.80 (s, 1H), 8.93 (d, *J* = 4.5 Hz, 2H); ^{13}C-NMR (125 MHz, Chloroform-*d*): δ (in ppm) 13.09, 19.78, 21.67, 26.07, 26.68, 29.18, 30.91, 31.74, 36.09, 42.33, 118.38, 119.69, 125.34, 128.37, 129.51, 129.85, 132.92, 140.48.

Porphyrin 4Pd: Orange solid, M.P. > 250 ^{O}C. Yield 85% (84 mg). $R_f = 0.30$ (DCM/ Hexane 1: 1.2), MALDI-MS for $C_{56}H_{23}F_{15}N_5Pd$ $[M+H]^+$ calcd 1156.0749 observed m/z 1156.83**.** IR (neat, cm^{-1}): 2954, 2912, 2835, 1580. ^{1}H-NMR (500 MHz, Chloroform-*d*): δ (in ppm) 7.10 (m, 3H), 7.37 (d, $J = 4.2$ Hz, 9H), 7.93 (d, $J = 8.4$ Hz, 2H), 8.72 (d, $J = 4.5$ Hz, 2H), 8.76 (m, 4H), 9.01 (d, $J = 4.7$ Hz, 2H); ^{13}C-NMR (125 MHz, Chloroform-*d*): δ (in ppm) 103.82, 119.75, 122.68, 124.22, 128.50, 128.58, 129.58, 129.91, 132.51, 132.74, 134.10, 140.11, 140.44.

General synthesis of carboxylic acids

The aldehydes (0.5 mmol) and 1 mL DCM solution of Pd(II) porphyrins (0.5 x 10^{-3} mmol) (**1Pd/2pd/3Pd/4Pd**) were dissolved in 14 mL of acetonitrile in a two neck round bottom flask. Reaction flask was fixed into a cardboard box in such a way that, it could be exposed to the light source (λ = 400-700 nm, 15 J cm^{-2}) and reaction was stirred at room temperature under oxygen atmosphere. Reaction was monitored by TLC (50% ethyl acetate/ pet-ether), the spot corresponding to the carboxylic acid was clearly visible on TLC under UV-lamp. The solvent was removed on rotary evaporator under vacuum and the crude product was purified by silica gel column chromatography in 50% ethyl acetate /pet-ether mixture. The conversion of aldehydes into carboxylic acid was measured by IR spectroscopy.

4-methylbenzoic acid: IR (neat, cm-1): 3384, 2922, 2855, 1547, 1399, 1085.

2,4,6-methylbenzoic acid: IR (neat, cm-1)3442, 2924, 2854, 1688, 1607, 1458.

2-nitrobenzoic acid: IR (neat, cm-1): 3450, 2920, 2855, 1695, 1526, 1456.

4-nitrobenzoic acid: IR (neat, cm-1): 3411, 2915, 2848, 1705, 1606, 1539.

References

[1] J. S. Lindsey, in *The Porphyrin Handbook*, ed. K. M. Kadish, K. M. Smith and R. Guilard, Academic Press, San Diego, 1 (2000) Chapter 2.

[2] L. R. Milgrom, *The Colours of Life-An Introduction to the Chemistry of Porphyrins and Related Compounds*, Oxford University Press, Inc.: New York, NY, USA, 22 (1997).

[3] M. O. Senge, S. A. MacGown, J. M. O'Brein, Chem. Commun. 51 (2015) 17031.

[4] J.C. Barona-Castano, C.C. Carmona-Vargas, T.J. Brocksom, K.T. De Oliveira, M. Graca, P.M.S. Neves, M. Amparo, F. Faustino, Molecules. 21 (2016) 310.

[5] M. Costas, Coord. Chem. Rev. 255 (2011) 2912.

[6] C.-C. Guo, X.-Q. Liu, Q. Liu, Y. Liu, M.-F. Chu, W.-Y. Lin, J. Porphyrins Phthalocyanines 13 (2009) 1250.

[7] C.-M. Che, J.-S. Huang, Chem. Commun. 27 (2009)3996.

[8] H. Srour, P. Le Maux, G. Simmonneaux, Inrog. Chem. 51 (2012) 5850.

[9] J. L. Zhang, H. B. Zhou, J. S. Huang, C. M. Che, Chem. Eur. J. 8 (2002) 1554.

[10] H.-B. Ji, Q.-L. Yuan, X.-T. Zhou, L.-X. Pei, L.-F. Wang, Biorg. Med. Chem. Lett. 17 (2007), 6364.

[11] M. Hajimohammadi, N. Safari, H. Mofakham, F. Deyhimi, Green Chem. 13 (2011) 991.

[12] M. Hajimohammadi, N. Safari, H. Mofakham, A. Shaabani, Tetrahedron Lett. 51 (2010) 4061.

[13] A. Maldotti, C. Bartocci, G. Varani, A. Molinari, P. Battioni, D. Mansuy, Inorg. Chem. 35 (2002) 1126.

[14] M. A. Faustino, M. G. Neves, J. A. Cavaleiro, M. Neumann, H. D. Brauer, G. Jori, Photohem. Photobiol. 72 (2000) 217.

[15] M. Hajimohammadi, N. Safari, J. Porphyrins Phthalocyanines 14 (2010) 639.

[16] H. R. Khavasi, N. Safari, J. Mol. Catal. A. 220 (2004) 127.

[17] P.E. Ellis, J. E. Lyons, Coord. Chem. Rev. 105 (1990) 181.

[18] M.R.Iesce, C. Flavio, F. Temussi, Curr. Org. Chem. 9 (2005) 109.

[19] G. Jiang, J. Chen., J. S. Huang, C.-M. Che, Org. Lett. 11 (2009) 4568.

[20] S. Das, H.R. Bhat, N. Balsukuri, P.C. Jha, Y. Hisamune, M. Ishida, H. Furuta, S. Mori, I. Gupta, Inorg. Chem. Front. 4 (2017) 618.

[21]S. Das, S., I. Gupta, J. Porphyrins Phthalocyanines. 23 (2019) 367.

[22] M. Gouterman, in *The Porphyrins*, ed. D. Dolphin, Academic Press: New York, Vol. 3 (1978) 1.

[23] I. Gupta, M. Ravikanth, J. Chem. Sci. 117 (2005) 161.

[24] N. Balsukuri, I. Gupta, Dyes Pigments 144 (2017) 223.

[25] N. Balsukuri, S. Das, I. Gupta, New J. Chem. 39 (2015) 482.

[26]M. Frisch, G. T., H. Schlegel, G. Scuseria, M. Robb, J. Cheeseman, G. Scalmani, V. Barone, B. Mennucci, G. Petersson, H. Nakatsuji, M. Caricato, X. Li, H. Hratchian, A.Izmaylov, J. Bloino, G. Zheng, J. Sonnenberg, M. Hada, M. Ehara, K. Toyota, R. Fukuda, J. Hasegawa, M. Ishida, T. Nakajima, Y. Honda, O. Kitao, H. Nakai, T. Vreven, J. A. Montgomery, Jr., J. Peralta, F. Ogliaro, M. Bearpark, J. Heyd, E. Brothers, K. Kudin, V. Staroverov, T. Keith, R. Kobayashi, J. Normand, K. Raghavachari, A. Rendell, J. Burant, S. Iyengar, J. Tomasi, M. Cossi, N. Rega, J. Millam, M. Klene, J. Knox, J. Cross, V. Bakken, C. Adamo, J. Jaramillo, R. Gomperts, R. Stratmann, O. Yazyev, A. Austin, R. Cammi, C. Pomelli, J. Ochterski, R. Martin, K. Morokuma, V. Zakrzewski, G. Voth, P. Salvador, J. Dannenberg, S. Dapprich, A. Daniels, O. Farkas, J. Foresman, J. Ortiz, J. Cioslowski, and D. Fox, , 09, Revision D. 01, Gaussian. *Inc., Wallingford, CT* **2009**.

[27] J. Zhang, C. Jiang, J.P. Figueiró Longo, R.B. Azevedo, H. Zhang, L.A. Muehlmann, Acta Pharm. Sin. B. 8 (2018) 137.

[28] P. R. Ogilby, Chem. Soc. Rev. 39 (2010) 3181.

[29] S. Singh, A. Aggarwal, N.V.S.D.K. Bhupathiraju, G. Arianna, K. Tiwari, C.M. Drain, Chem. Rev. 115 (2015) 10261.

[30] M.K. Raza, S. Gautam, A. Garai, K. Mitra, P. Kondaiah, A.R. Chakravarty, Inorg. Chem. 56 (2017) 11019.

[31] P. Pushpanandan, Y.K. Maurya, T. Omagari, R. Hirosawa, M. Ishida, S. Mori, Y.

Yasutake, S. Fukatsu, J. Mack, T. Nyokong, H. Furuta, Inorg. Chem. 56 (2017) 12572.

[32] M. Hajimohammadi, H. Mofakham, N. Safari, A.M. Manesh, J. Porphyrin Phthalocyanines 16 (2012) 93.

[33] I. Kruk, A. E. Hassan, T. Michalaska, K. Ichszteld, K. Kubasik-Kladna, S. Olgen, Luminescence 22 (2007) 379.

Pd(II) porphyrins: Synthesis, singlet oxygen generation and photoassisted oxidation of aldehydes to carboxilic acids

Vijayalakshmi Pandey,[a] Drishti Jain,[a] Nitesh Pareekh[a] and Iti Gupta*[a]

Indian Institute of Technology Gandhinagar, Village Palaj, Simkheda, Gandhinagar, Gujarat-382355, India. *Corresponding author, e-mail: iti@iitgn.ac.in

Highlights

- Synthesis and optical studies of A_3B and A_2B_2 type porphyrins and their Pd(II) complexes is reported.
- The *meso*-positions on porphyrin macrocycle are substituted with pentafluorophenyl and *N*-butylcarbazole or triphenylamine groups, for better catalytic activity.
- Pd(II) porphyrins displayed decent phosphorescence ~670 nm and generated singlet oxygen by type II pathway, after photoirradiation.
- The catalytic application of Pd(II) porphyrins towards photoassisted aerobic oxidation of aromatic aldehydes to carboxylic acids is demonstrated.

Authors state that, all co-authors have seen and approved the final version of the manuscript being submitted. Authors warrant that the article is our original work, which has not received prior publication and is not under consideration for publication elsewhere.

Declaration of interests

☒ The authors declare that they have no known competing financial interests or personal relationships that could have appeared to influence the work reported in this paper.

☒The authors declare the following financial interests/personal relationships which may be considered as potential competing interests:

Authors declare no conflict of interest.

Authors declare no financial interest.